

## Twinning and superstructure of Al-rich mullite

YOSHIHARU NAKAJIMA AND PAUL H. RIBBE

Department of Geological Sciences  
Virginia Polytechnic Institute and State University  
Blacksburg, Virginia 24061

### Abstract

Submicroscopic (001) twinning on a scale of 20–100 nm has been observed by transmission electron microscopy in synthetic Al-rich mullite,  $Al_2^i[Al_{2+2x}Si_{2-2x}]^vO_{10-x}$  ( $x \sim 0.55$ ), using dark-field, SAED, and lattice imaging techniques. Diffraction maxima from the twinned mullite subcells exactly superpose in the  $h0l$  net, but the non-rational 'e' and 'f' satellite reflections do not, giving the appearance of a "second antiphase domain structure parallel to  $c^*$ " (Cameron, 1977). In fact, in an untwinned segment of this mullite there is only one set of antiphase domain boundaries (APB's) in non-rational orientations. These domains are related by  $\frac{1}{2}[001]$  across APB's, and since in ( $h0l$ ) projection they are, on the average,  $B$ -face-centered ( $c = 5.8\text{\AA}$ ), they give rise to the odd-order 'e' reflections and even-order 'f' reflections, analogous to 'e' and 'f' reflections in plagioclase feldspars. The magnitude of the vector  $S$ , joining an 'e', satellite reflection to the position of the absent  $h$ -odd,  $l$ -odd diffraction, is composition-dependent (Cameron, 1977), but the orientation of  $S$  apparently shifts from parallel to  $a^*$  (for  $x < 0.5$ ) to one with an increasing  $c^*$  component (for  $x > 0.5$ ). Ordered oxygen vacancies are presumed responsible for the periodic modulation of magnitude  $1/|2S|$  in the non-rational plane normal to  $S$ . Double diffraction accounts for the multitude of additional weak diffraction maxima observed in electron diffraction patterns (but not in X-ray patterns) from twinned crystals. Untwinned crystals do not exhibit double diffraction.

### Introduction

In a systematic crystallographic study Cameron (1977) concluded that complete solid solution probably exists between mullite ( $Al_{4+2x}Si_{2-2x}O_{10-x}$ ) and sillimanite ( $Al_4Si_2O_{10}$ ;  $x = 0$ ), where  $x$  for mullite has an observed range of 0.17 to 0.59. Lattice parameters vary almost linearly with  $x$ , the  $a$  and  $b$  cell dimensions converging near  $x \sim 0.65$ . Density decreases with  $x$ , and Cameron (1977, his Fig. 1) demonstrated conclusively that increasing oxygen vacancies are responsible for the decrease, with the total number of Al + Si atoms constant at six. Extrapolation of lattice parameters and densities of this series to  $x = 1.0$  (zero Si), led Cameron to suggest that the unstable phase known as  $\iota$ - $Al_2O_3$  (iota alumina) may be an end-member of a sillimanite–mullite–alumina series across which vacancies at the O3 oxygen site charge-balance the substitution of tetrahedral Al for Si:  $2Al^{3+} + \square = 2Si^{4+} + O^{2-}$ .

The oxygen vacancies are highly ordered in mul-

lite, producing an incommensurate antiphase domain structure. Because of the marked similarities of superlattice 'e' and 'f' reflections to those in plagioclase feldspars,  $Na_{1-z}Ca_zAl_{1+z}Si_{3-z}O_8$ , Smith and McConnell (1966) recognized that the mullite superstructures were at least *geometrically* analogous to the domain structures of intermediate plagioclases with  $0.25 < z < 0.75$  (*cf.* Bown and Gay, 1958). It would appear that up to  $x \sim 0.5$ , the antiphase domain boundaries (APB's) in mullite are oriented normal to  $a^*$ . The displacement vector is  $\frac{1}{2}[001]$  between adjacent domains, where  $c = 2 \times 2.9\text{\AA}$  (Nakajima *et al.*, 1975). Cameron (1977) measured the vector  $s$ , which is defined by joining an 'e,' satellite reflection to the position of the systematically absent  $h$ -odd,  $l$ -odd diffraction (see Fig. 1), and he found that the  $1/|2s|$  periodicity of the superstructure increases more or less linearly with  $x$ , at least up to  $x = 0.47$  (his Fig. 4). In fact (as we shall see) when his data are properly interpreted, the linearity of  $1/|2s|$  vs.  $x$  persists up to  $x$

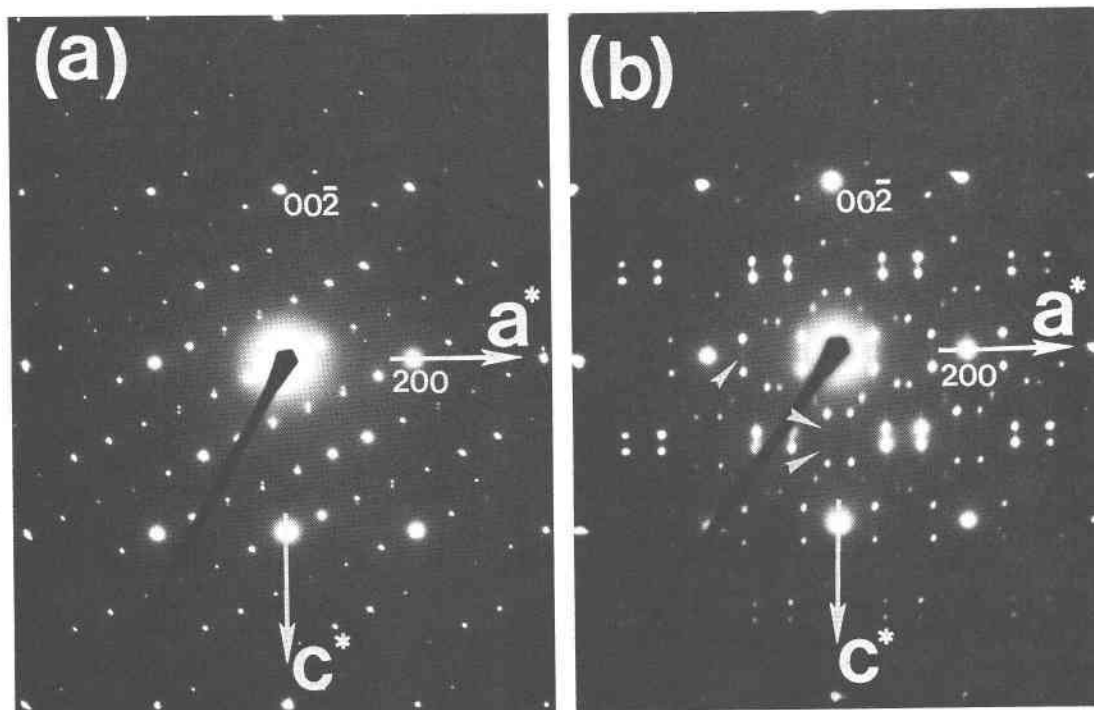


Fig. 1. Selected-area electron diffraction (SAED) patterns for high-alumina mullite: (a) untwinned (b) twinned on (001) plane. The incident electron beam is normal to (010). Some of the double diffraction spots are marked by arrowheads.

= 0.59, although, ironically, our specimen does not fall on the line.

Cameron also observed that selected area electron diffraction patterns (SAED's) of synthetic high-alumina mullites ( $x > 0.5$ ) quenched above 2100°C showed additional superstructure reflections; his Figures 3f and 3g are comparable to Figure 1b. From these he hypothesized "a second antiphase domain structure parallel to  $c^*$ " superposed on the first, which is parallel to  $a^*$  (the APB's would be normal to  $c^*$  and  $a^*$ , respectively).

Using high-alumina mullite crystals (82 wt%  $\text{Al}_2\text{O}_3$ ) synthesized by Dr. W. M. Kriven<sup>1</sup> in a manner similar to that used by Cameron, we have found that the complexities of the SAED's may actually be explained by (001) twinning and double reflection. We have observed both ion-thinned and powdered mullites by high-resolution transmission electron microscopy (HRTEM) at 100 kV, using a JEOL 100C elec-

tron microscope equipped with a side-entry eucentric goniometer.

### Observations and discussion

#### Composition

The bulk composition of the starting materials was 82 wt%  $\text{Al}_2\text{O}_3$ , 18 wt%  $\text{SiO}_2$ , which calculates to  $\text{Al}_{5.06}\text{Si}_{0.94}\text{O}_{9.47}$ ,  $x = 0.53$ . However, on the mullite crystals we observed, *in situ* energy dispersive X-ray analysis in the transmission microscope indicated a composition for the mullite of  $\text{Al}_{5.14}\text{Si}_{0.86}\text{O}_{9.43}$ ,  $x = 0.57$ . Although this value is very close to that which one would deduce by comparing the unit-cell parameters [ $a = 7.62$ ,  $b = 7.66$ ,  $c = 2.89\text{Å}$  (*esd*  $\pm 0.02\text{Å}$ )] measured from X-ray precession photographs, with the graphs of  $a$ ,  $b$ , and  $c$  vs.  $x$  in Figure 2 of Cameron (1977, p. 750), the precision of both methods is limited. In fact, small amounts of alumina and a glassy phase which may be silica are finely dispersed in this mullite. Thus, in order not to give inordinate weight to any determinative method, we have designated an approximate composition ( $x \sim 0.55$ ) for this specimen half-way between that of the batch material and the X-ray analysis.

<sup>1</sup>Finely ground mixtures of  $\text{Al}_2\text{O}_3$  and fused silica were sealed in a molybdenum tube and homogenized for 24 hours at 2100°C and then quenched to room temperature (Kriven and Pask, in preparation).

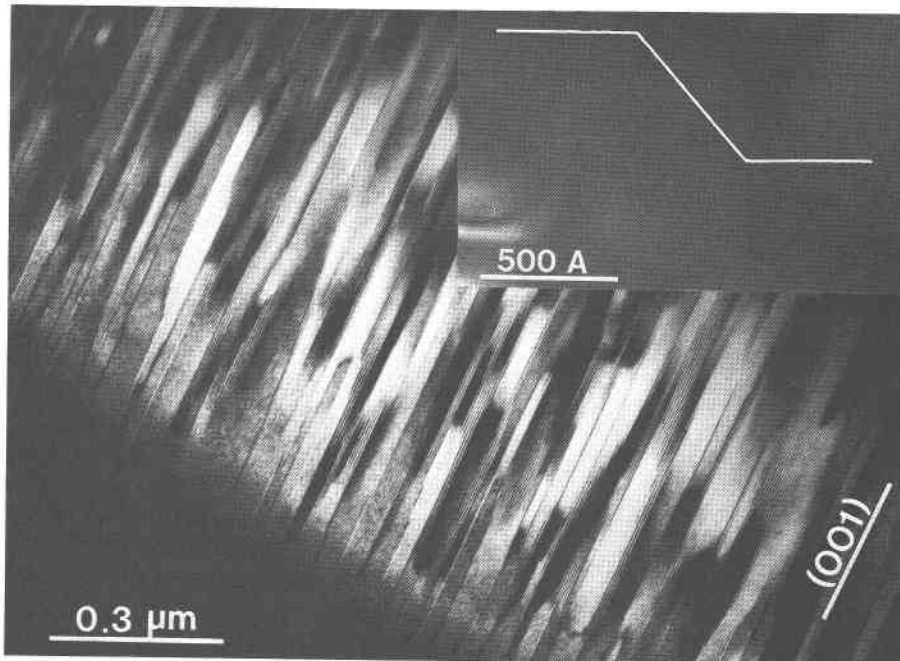


Fig. 2. Twin texture of high-alumina mullite shown in a dark-field electron micrograph obtained by imaging 'e' satellite reflections only. The inset is a high resolution many-beam lattice image showing lattice fringes of  $\sim 13\text{\AA}$  spacing corresponding to that of the APB's. Note: wide fringes along twin boundaries in the dark-field image are parallel Moiré patterns.

### Twinning

Figure 1 contains selected area electron diffraction (SAED) patterns for both untwinned and twinned portions of this Al-rich mullite. A dark-field image of the (001) twins (Fig. 2) shows somewhat irregular lamellar units 20–100 nm thick. The high-resolution

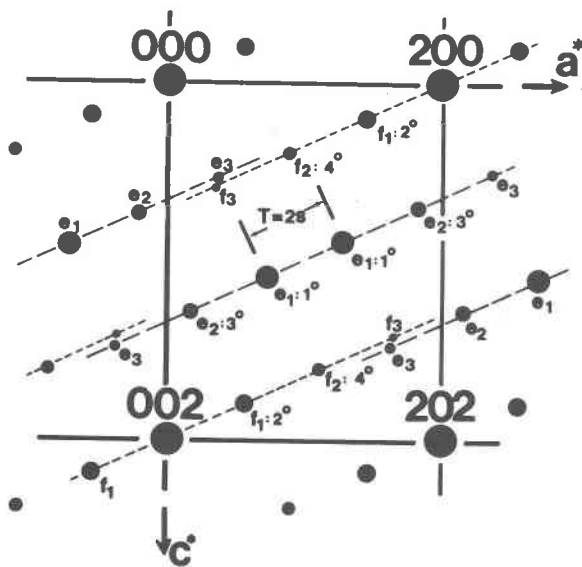


Fig. 3. Indexed schematic diffraction pattern of untwinned Al-rich mullite corresponding to Fig. 1a.

lattice image in the inset shows two strained interfaces parallel to the (001) twin plane. The superlattice 'e' and 'f' reflections, labeled in a schematic drawing in Figure 3 and shown in the  $h0l$  plane in Figure 1a, lack the apparent  $mm$  symmetry of those in the twinned pattern (Fig. 1b). This is consistent with the observation by Tokonami *et al.* (1980) that the true mullite supercell, produced by ordered oxygen vacancies, is triclinic. Very weak streaks parallel to  $c^*$  through all reflections in the SAED pattern of the twinned mullite are undoubtedly due to the irregular thicknesses of the (001) twin lamellae and in some degree to their strained and somewhat irregular subparallel interfaces. Thus we conclude that the appearance of a "second antiphase domain structure parallel to  $c^*$ " at values of  $x$  greater than 0.5 (Cameron, 1977, p. 751) is caused by twinning.

Although the origin of twinning in mullite with  $x > 0.5$  is not understood, it may be the result of a phase transformation from a cell with orthogonal geometry for the disordered phase at high temperatures to a triclinic cell whose lower symmetry results from the ordering of oxygen vacancies. The parallel Moiré patterns observed at many twin interfaces (Fig. 2) suggest the possibility of some structural distortion and/or compositional variation along the (001) boundaries.

### Double diffraction

Figure 1b and Cameron's Figures 3f and 3g show a multitude of very weak diffraction maxima in addition to the expected 'e' and 'f' reflections in (001) twinned mullite. These are absent in SAED patterns of untwinned high-alumina mullite (Fig. 1a) and in X-ray precession photographs of twinned material (Fig. 4). The conclusion is that in this mullite and Cameron's Al-rich specimens, Q1 and Q2, electron beams (but not X-ray beams) diffracted from one set of small domains pass into twin-related ones where they are diffracted a second time (see Hirsch *et al.*, 1977, chapters 5 and 6). This may be substantiated by deflecting the direct beam alternately to the positions of the intense twin-related 'e<sub>1</sub>' satellite reflections, which generates the entire set of secondary weak diffraction maxima, some of which superpose on primary satellite reflections from the (001) twins.

### Antiphase domains

The antiphase structure of mullite was imaged with HRTEM by Nakajima *et al.* (1975, Fig. 2). It was presumed due to ordering of the oxygen vacancies and tetrahedral Al atoms in partially-occupied tetrahedral sites. Agrell and Smith (1960) summarized the phenomena of satellite reflections in mullite, and Tokonami *et al.* (1980) proposed an elaborate model to account for all kinds of subsidiary reflections, including the extinction rules observed among the odd-order 'e' satellite reflections, disposed on a line through systematically absent reflections with indices *l*-odd, and the even-order 'f' satellites, disposed along a line through *l*-even reflections from the  $c = 5.8\text{\AA}$  cell (see Fig. 3). Their model supersedes those of Guse and Saalfeld (1976) and Saalfeld (1979).

To be consistent with symbols used for satellite reflections in the intermediate plagioclases, the 'e' reflections are labeled 'e<sub>i</sub>' ( $i = 1, 2, 3, \dots$ ) and correspond to first, third, fifth,  $\dots$ -order reflections. The 'f' reflections are labeled 'f<sub>j</sub>' ( $j = 1, 2, 3, \dots$ ) and correspond to second, fourth, sixth,  $\dots$ -order reflections. The extinctions are proof that the average structure related across APB's is "pseudo"-*B*-face-centered: *h*-odd, *l*-odd diffraction maxima are absent in the *h0l* net and have been replaced by 'e' satellites symmetrically disposed about that point in the *h0l* reciprocal net. Their attendant 'f' satellites are symmetrically disposed about the *h*-even, *l*-even diffraction maxima of the mullite subcell [*cf.* Figs. 3 and 5; see Korekawa (1967), Jamieson *et al.* (1969) and Böhm (1975, 1976) for diffraction theory of satellite

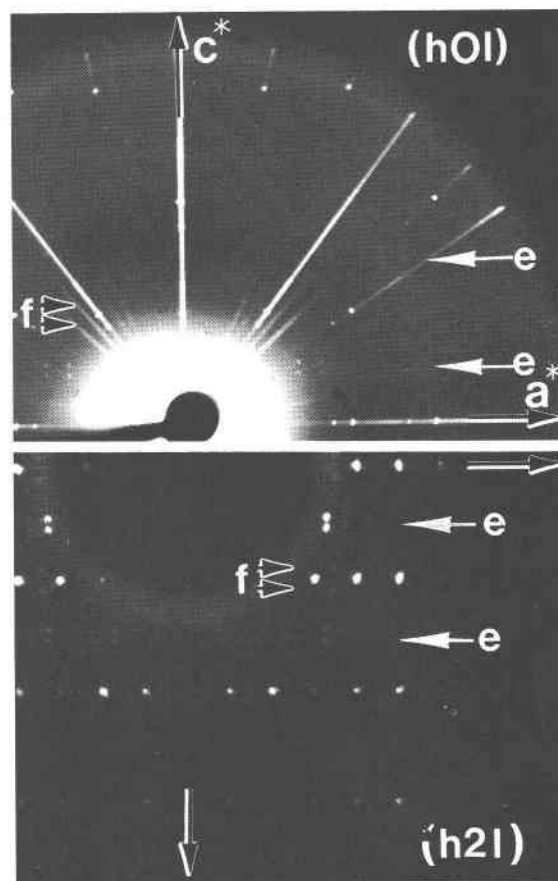


Fig. 4. *h0l* and *h2l* X-ray precession photographs (Zr-filtered Mo radiation) of a twinned high-Al mullite. 'e' and 'f' reflections are indicated; no additional reflections due to double diffraction are observed (*cf.* Fig. 1b).

reflections and Smith (1974, Ch. 5) for application to the plagioclases].

Above  $x = 0.5$ , the vector *S*, joining an 'e<sub>1</sub>' satellite reflection to the position of the absent *h*-odd, *l*-odd diffraction in the *h0l* net, shifts from an orientation parallel to *a*\* at values of  $x < 0.5$  to one with an increasing *c*\* component as  $x$  increases (see Fig. 3, and *cf.* Cameron's Fig. 3). Cameron had hypothesized a second antiphase domain structure to explain the doubling of the satellite reflections in the *c*\* direction, thus overlooking both the existence of (001) twins and the fact that the *S* vectors for his Al-rich specimens were shorter than anticipated. His data are replotted in Figure 6 where  $1/|2S|$ , the periodicity of the antiphase superstructure, is seen to increase more or less regularly from  $x = 0.25$  to 0.59. The scatter of two Al-poor specimens (92423 and Al-37y) from the curve was attributed by Cameron to marked differences in thermal history, and this ultimately may

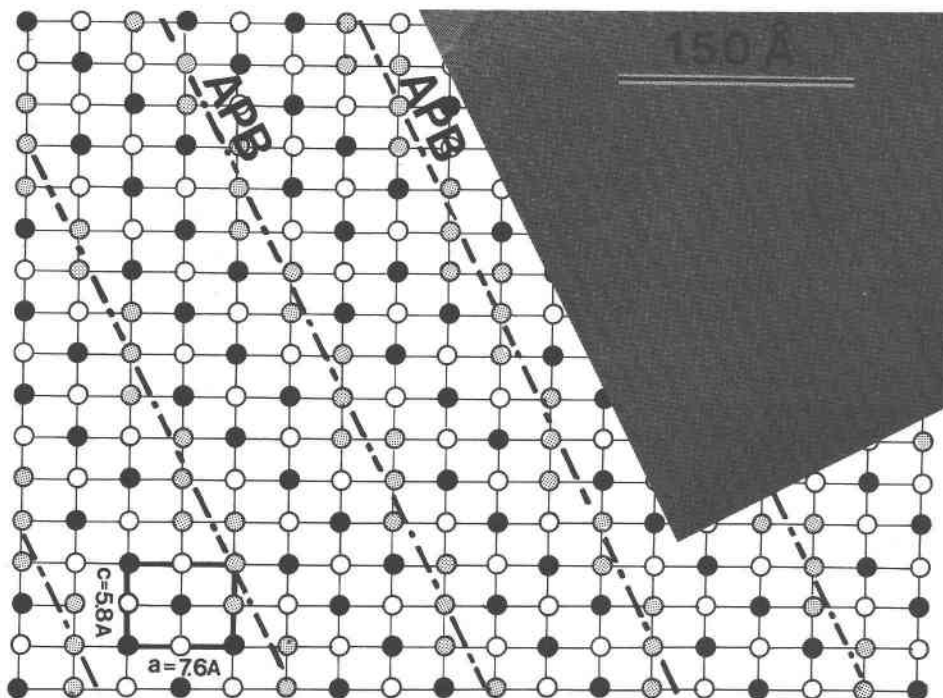


Fig. 5. Superstructure model and properly oriented high-magnification lattice image for high-alumina mullite. Details are discussed in the text.

prove to be the reason for the departure of our Al-rich specimen from the curve. In our specimen  $s$  is nearly parallel to  $[301]^*$ , and the APB repeat normal to that direction is  $\sim 12.8\text{\AA}$  (cf. Fig. 5).

Although it is not certain why the APB's retain

their (100) orientation up to  $x = 0.5$ , the fact that they "migrate" to non-rational orientations with composition above  $x = 0.5$  is not unique, having been reported in plagioclases (Bown and Gay, 1958) and in NA type pyrrhotite (Nakazawa *et al.*, 1976).

In sillimanite ( $x = 0$ ) tetrahedral Al and Si are perfectly ordered in the double chain which has a  $c$ -repeat of  $5.8\text{\AA}$  (Winter and Ghose, 1979; Peterson and McMullen, 1980). But in mullite ( $0.19 < x < 0.59$ ) the substitution  $2\text{Al}^{3+} + \square \rightarrow 2\text{Si}^{4+} + \text{O}^{2-}$  with increasing  $x$  requires a disordering of Al and Si in the average structure, resulting in a  $c$  dimension of  $\sim 2.9\text{\AA}$ . Ever since the determination of the average structure (Sadanaga *et al.*, 1962; Durovic, 1962; Burnham, 1963, 1964), the origin of the superstructure in mullite has been presumed due to ordering of oxygen vacancies among the O3 sites in adjacent subcells and a concurrent movement of some of the Al into a new tetrahedral site (designated Al\* by Burnham, 1963) which is only partially occupied. Inasmuch as no sharp satellite reflections appear in  $hk0$  and  $0kl$  diffraction patterns, we assume that the superstructure is two-dimensional.

In agreement with the interpretation of the superstructure by Nakajima *et al.* (1975) and Tokonami *et al.* (1980), we have drawn in Figure 5 a model of the

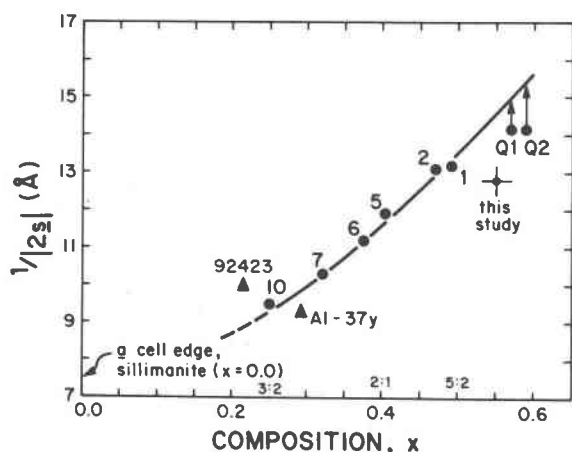


Fig. 6. A plot of  $1/|2s|$ , the periodicity of the superstructure, vs.  $x$  in the mullite formula  $\text{Al}_{4+2x}\text{Si}_{2+2x}\text{O}_{10-x}$ . Numbered specimens (dots and triangles) are from Cameron (1977, Fig. 4). Arrows indicate increase in  $s$  values where the  $c^*$  component was taken into account for Q1 and Q2. The specimen of this study is represented by a cross with approximate error bars.

antiphase domains with non-rational APB's which is consistent with symmetry constraints in accord with satellite extinction rules, with the  $\frac{1}{2}[001]$  fault vector, and with the high-resolution TEM image of our high-Al mullite (Fig. 5 inset). Plotting in the  $[010]$  projection only the O3 sites, a regular array of vacancies (open circles), of which there must be two per unit cell at  $x = 0.5$ , alternates with fully occupied sites (filled circles). Partially occupied O3 sites are assumed to occur along the APB's. In this drawing fourth rows of O3 sites parallel to  $c$  are related to one another by  $\frac{1}{2}[001]$ , where  $c = 5.8\text{\AA}$  on the pseudo- $B$ -centered cell. A change in the proportion of filled O3 sites will change the ordered pattern and shift the APB's. The effects of heat treatment and quenching rates on these phenomena remain to be explored.

### Acknowledgments

We thank Professor J. A. Pask and Dr. W. M. Kriven for providing the specimen, Professor N. Morimoto and Dr. M. Tokonami for helpful discussions, and Dr. G. L. Nord for his critical review. Financial support was provided in part by NSF grant EAR77-23114 to PHR and G.V. Gibbs.

### References

- Agrell, S. O., and Smith, J. V. (1960) Cell dimensions, solid solution, polymorphism, and identification of mullite and sillimanite. *Journal of the American Ceramic Society*, 43, 69-76.
- Böhm, H. (1975) Interpretation of X-ray scattering patterns due to periodic structural fluctuations. I. The case of transverse modulation of positional parameters in primitive lattices. *Acta Crystallographica*, A31, 622-628.
- Böhm, H. (1976) Interpretation of X-ray patterns due to modulation of positional parameters and of scattering density. *Zeitschrift für Kristallographie*, 143, 56-66.
- Bown, M. G. and Gay, P. (1958) The reciprocal lattice geometry of the plagioclase feldspar structure. *Zeitschrift für Kristallographie*, 111, 1-14.
- Burnham, C. W. (1963a) Crystal structure of mullite. *Carnegie Institution of Washington Year Book*, 62, 223-227.
- Burnham, C. W. (1963b) Composition limits of mullite, and the sillimanite-mullite solid solution problem. *Carnegie Institution of Washington Year Book*, 62, 227-228.
- Cameron, W. E. (1977) Mullite: a substituted alumina. *American Mineralogist*, 62, 747-755.
- Durovic, S. (1962) A statistical model for the crystal structure of mullite. *Kristallografiya*, 7, 339.
- Guse, W. and Saalfeld, H. (1976) Das diffuse Beugungsbild von Mullit,  $2\text{Al}_2\text{O}_3 \cdot \text{SiO}_2$ . *Zeitschrift für Kristallographie*, 143, 177-187.
- Hirsch, P., Howie, A., Nicholson, R. B., Pashley, D. W., and Whelan, M. J. (1977) *Electron Microscopy of Thin Crystals*. Robert E. Krieger Publishing Co., Huntington, New York.
- Jamieson, P. B., De Fontaine, D., and Abrahams, S. C. (1969) Determination of atomic ordering arrangements from a study of satellite reflections. *Journal of Applied Crystallography*, 2, 24-30.
- Korekawa, M. (1967) *Theorie der Satellitenreflexe*. Habilitationsschrift der Ludwig-Maximilians-Universität, München.
- Nakajima, Y., Morimoto, N., and Watanabe, E. (1975) Direct observation of oxygen vacancy in mullite  $1.86\text{Al}_2\text{O}_3 \cdot \text{SiO}_2$ , by high resolution electron microscopy. *Proceedings of the Japan Academy*, 51, 173-178.
- Nakazawa, H., Morimoto, N., and Watanabe, E. (1976) Direct observation of iron vacancies in polytypes of pyrrhotite. In H. R. Wenk, Ed., *Electron Microscopy in Mineralogy*, p. 304-309. Springer-Verlag, New York.
- Peterson, R. and McMullen, R. K. (1980) Neutron structure refinements of the  $\text{Al}_2\text{SiO}_5$  polymorphs. *Transactions of the American Geophysical Union*, EOS, 61, 409.
- Saalfeld, H. (1979) The domain structure of 2:1-mullite ( $2\text{Al}_2\text{O}_3 \cdot \text{SiO}_2$ ). *Neues Jahrbuch für Mineralogie, Abhandlungen*, 134, 305-316.
- Sadanaga, R., Tokonami, M., and Takéuchi, Y. (1962) The structure of mullite,  $2\text{Al}_2\text{O}_3 \cdot \text{SiO}_2$ , and relationship with the structures of sillimanite and andalusite. *Acta Crystallographica*, 15, 65-68.
- Smith, D. G. W. and McConnell, J. D. C. (1966) A comparative electron diffraction study of sillimanite and some natural and artificial mullites. *Mineralogical Magazine*, 35, 810-814.
- Smith, J. V. (1974) *Feldspar Minerals, Volume 1*. Springer-Verlag, New York.
- Tokonami, M., Nakajima, Y., and Morimoto, N. (1980) Diffraction aspect and a structural model of mullite,  $\text{Al}(\text{Al}_{1+2x}\text{Si}_{1-2x})\text{O}_{5-x}$ . *Acta Crystallographica*, A36, 270-276.
- Winter, J. K. and Ghose, S. (1979) Thermal expansion and high-temperature crystal chemistry of the  $\text{Al}_2\text{SiO}_5$  polymorphs. *American Mineralogist*, 64, 573-586.

*Manuscript received, April 9, 1980;  
accepted for publication, August 19, 1980.*